Ocean Sci. Discuss., https://doi.org/10.5194/os-2019-46
Manuscript under review for journal Ocean Sci.
Discussion started: 20 May 2019

Ocean Science
Discussions
Open Access

Implications of different nitrogen input sources for potential production and carbon flux estimates in the coastal Gulf of Mexico (GOM) and Korean coastal waters

Jongsun Kim,[a,*] Piers Chapman,[a,*] Gilbert Rowe [a, b], and Steven F DiMarco [a]

[a] Department of Oceanography, Texas A&M University, College Station, TX 77843-3146, USA

[b] Department of Marine Biology, Texas A&M University, Galveston, TX 77553, USA

[*] Corresponding authors

*J. Kim. Email: jongsun@tamu.edu.

*P. Chapman. Email: piers.chapman@tamu.edu.

Ocean Sci. Discuss., https://doi.org/10.5194/os-2019-46
Manuscript under review for journal Ocean Sci.
Discussion started: 20 May 2019

Abstract

The coastal Gulf of Mexico (GOM) and Coastal Sea off Korea (CSK) both suffer from human-induced eutrophication. We used a N-mass balance model in two different regions with different nitrogen input sources to estimate organic carbon fluxes and predict future carbon fluxes under different model scenarios. The coastal GOM receives nitrogen predominantly from the Mississippi and Atchafalaya Rivers and atmospheric nitrogen deposition (AN-D) is only a minor component in this region. However, in the CSK, groundwater and atmospheric nitrogen deposition are more important controlling factors. Our model includes the fluxes of nitrogen to the ocean from the atmosphere, groundwater, and rivers, based on observational and literature data, and identifies three zones (brown, green and blue waters) in the coastal GOM and CSK with different productivity and carbon fluxes. Based on our model results, the potential primary production rate in the inner (brown water) zone are more than 2 (GOM) and 1.5 gC m^{-2} day^{-1} (CSK). In the middle (green water) zone, potential production is between 0.1 to 2 (GOM) and 0.3 to 1.5 gC m^{-2} day^{-1} (CSK). In the offshore (blue water) zone, productivity is less than 0.1 (GOM) and 0.3 (CSK) gC m^{-2} day^{-1}. Through our model scenario results, overall oxygen demand in the GOM would increase approximately 21% if we fail to reduce riverine N input, likely increasing considerably the area affected by hypoxia. Comparing the results from the U.S. with those from Korea shows the importance of considering both riverine and atmospheric inputs of nitrogen. This has direct implications for investigating how changes in energy technologies can lead to changes in the production of various atmospheric contaminants that affect air quality, climate and the health of local populations.

Keywords:

Ocean Sci. Discuss., https://doi.org/10.5194/os-2019-46
Manuscript under review for journal Ocean Sci.
Discussion started: 20 May 2019

Ocean Science
Discussions

Chemical tracers, Biological processes, Shelf-seas, Gulf of Mexico, Yellow Sea.

Ocean Sci. Discuss., https://doi.org/10.5194/os-2019-46
Manuscript under review for journal Ocean Sci.
Discussion started: 20 May 2019

Introduction

Industrial expansion and anthropogenic emissions are major factors leading to increased coastal productivity and potential eutrophication (Sigman and Hain 2012). Coastal primary production is controlled largely by nitrogen (N) and phosphorous (P), and the relative supply of each determines which element limits production (Paerl 2009); freshwater inputs and the distance from sources such as river mouths are also important (Dodds and Smith 2016). Most coastal regions are N-limited, however, at certain times conditions can change from N-limited to P-limited (Dodds and Smith 2016; Howarth and Marino 2006). Sylvan et al. (2006), for example, suggested that the coastal GOM, especially near the Mississippi River delta mouth, is P-limited at certain times. Changes in nutrient loading from air-borne, river-borne and groundwater sources can also affect which element limits coastal productivity (Sigman and Hain 2012).

Several studies have shown that increasing atmospheric nitrogen deposition (AN-D) is known to contribute to ocean production globally, including eutrophication, while being of potential future importance in the GOM (Cornell et al., 1995; Doney et al., 2007; Duce et al., 2008; He et al., 2010; Kanakidou et al., 2016; Kim 2018; Kim (TW) et al., 2011; Lawrence et al., 2000; Paerl et al., 2002). Recently, Kim (TW) et al. (2011), using a model simulation showed that AN-D controls approximately 52% of the coastal productivity in the Yellow Sea. Global NOx emissions have increased but appear to be changing differently in the US and Asia (Kim (JY) et al., 2010; Luo et al., 2014; Shou et al., 2018; Zhao et al., 2015), and may affect not only coastal productivity but also global total nitrogen budgets. This study uses a box model to define potential carbon fluxes based on different nitrogen input sources in two different regions, the Coastal Gulf of Mexico (GOM) and the Coastal Sea off Korea (CSK).

Ocean Sci. Discuss., https://doi.org/10.5194/os-2019-46
Manuscript under review for journal Ocean Sci.
Discussion started: 20 May 2019

Most previous model studies in the GOM have been used to predict the size of the hypoxic zone (e.g., Fennel et al., 2006, 2011, 2013; Green et al., 2008; Hetland and DiMarco 2008; Justic et al., 2002; Rowe et al., 2002; Scavia et al., 2004; Turner et al. 2006, 2008), although Bierman et al. (1994), used a mass balance model to estimate carbon flux and oxygen exchange. The mass balance model is a useful tool to calculate nutrient or carbon fluxes and to estimate production in the coastal ocean (Kim (JS) et al, 2010; Kim (G) et al., 2011). All previous models for the GOM and the CSK have considered only riverine N as the predominant input source, and no one has considered AN-D as an input source to these regions.

In this study, we aimed to: 1) build a mass balance model considering not only riverine N input but also air-borne and groundwater-borne N; 2) use it to calculate potential primary production in the three regions defined by Rowe and Chapman (2002, henceforth RC02, see next section) and their associated coastal productivity; and 3) use the mass balance model to test the RC02 hypothesis. Because RC02 did not quantify their model with nutrient data and no one has applied this model to another region, we tested the RC02 hypothesis using data from both the GOM and the CSK that include low salinity samples. We used historical data from the mid-western and southern parts of the CSK and evaluated the theoretical model of RC02 in both areas where freshwater with high terrestrial input mixes into the coastal ocean.

Study areas

The Texas-Louisiana (LATEX) shelf in the northern Gulf of Mexico (GOM) has been affected by coastal nutrient loading, leading to hypoxia, coming from two major terrestrial sources (the Mississippi and Atchafalaya Rivers that together form the Mississippi-Atchafalaya River System MARS), that have different nutrient concentrations. The Gulf of Mexico (GOM) is a semi-enclosed oligotrophic sea and the MARS is the major source of nutrients and freshwater to the northern GOM (Alexander et al., 2008; Rabalais et al., 2002; Robertson and Saad, 2014). The MARS drains 41% of the contiguous United States (Milliman and Meade, 1983) and discharges approximately 20,000 m^3 s^{-1}, or about 60% of the total freshwater flow, to the northern side of the GOM (about 10.6 x 10^{11} m^3 $year^{-1}$ or 3.4 x 10^4 m^3 s^{-1}). The remainder comes from other U.S. rivers, Mexico and Cuba (Nipper et al., 2004).

At the Old River Control Structure on the lower Mississippi River approximately 25% of the Mississippi River's water is diverted into the Atchafalaya River, where it mixes with the water in the Red River. The flow in the Atchafalaya River totals 30% of the total MARS flow (Figure 1a). Several projects have investigated the relationship between nutrients and the marine ecosystem, and how this leads to hypoxia in the GOM (e.g. Bianchi et al., 2010; Diaz and Rosenberg, 1995, 2008; Forrest et al., 2011; Hetland and DiMarco, 2008; Laurent et al., 2012; Quigg et al., 2011; Rabalais and Smith, 1995; Rabalais et al., 2007; Rabalais and Turner 2001; Rowe and Chapman 2002). Strong stratification due to the high amount of freshwater discharged from the MARS, winds and nitrate concentration all affect hypoxia formation, with upwelling-favorable wind facilitating its development (Feng et al., 2012, 2014).

In the Northern GOM, the major factor controlling coastal productivity is riverine N input. Rowe and Chapman (2002), defined three theoretical zones over the LATEX shelf close to the Mississippi and Atchafalaya River mouths to predict the effects of nutrient loading on hypoxia along the river plumes and over the shelf. They named these the brown, green, and blue zones (Figure 2). Nearest the river mouths is a 'brown' zone, where the nutrient concentrations are high, but the discharge of sediment from the river reduces light penetration and limits primary productivity within the plume. Further away from the river plume, is a stratified 'green' zone with available light and nutrients that result in high productivity. In this region, the rapid depletion of nutrients is due to biological uptake processes that depend on the season and river flow (Bode and Dortch, 1996; Dortch and Whitledge, 1992; Lohrenz et al., 1999; Turner and Rabalais, 1994). Still further offshore, and also along the river plume to the west, there is the so-called 'blue' zone, defined arbitrarily by nitrate concentrations of 1 μM L^{-1} or less, which is dominated by intense seasonal stratification and a strong pycnocline, so that in the surface layer nutrients are limiting at this distance from the rivers and most primary production is fueled by recycled nutrients (Dortch and Whitledge, 1992). RC02 points out that the edges of the zones (geographical regimes) change over time depending on season, river flow, and biological processes (Figure 2).

The coastal sea off western Korea (CSK) forms the eastern side of another semi-enclosed basin (the Yellow Sea) and is affected by freshwater discharge from river plumes in the same way as the coastal GOM, although the freshwater flow is considerably less. The Yellow Sea covers about 380,000 km^2 area with an average water depth of 44m, and numerous islands are located on its eastern side (Liu et al., 2003). Our specific study area is the mid-western coastal region (MCK) from the Taean Peninsula to Gomso Bay (Figures 1c and 1d).

There is a strong tidal front in the coastal area near the Taean Peninsula due to sea floor topography and the coastal configuration (Park, 2017; Park et al., 2017). The region also contains several bays (Garolim Bay, Gomso Bay and Cheonsu Bay), and is affected by discharges from a large artificial lake (Saemangeum lake) and a freshwater discharge from the Keum river plume that contains high concentrations of nutrients (Lim et al., 2008). Conditions in the MCK near the Taean peninsula are similar to the coastal GOM, because of mixing of two different water masses from Gyunggi Bay (Han River) and the Keum River (Choi et al., 1998, 1999). The annual mean

Ocean Sci. Discuss., https://doi.org/10.5194/os-2019-46
Manuscript under review for journal Ocean Sci.
Discussion started: 20 May 2019

flow rate within the Keum River and precipitation within the catchment were about 70 m^3 s^{-1} (normal period), 170 m^3 s^{-1} (flood period) and 1,208 mm $year^{-1}$ during 2003 to 2005 (Yang and Ahn 2008).

Unlike the coastal GOM, the CSK has increased nitrogen inputs from atmospheric nitrogen deposition (AN-D) (the AN-D is approximately ten times higher than in the GOM, Table 2) (Kim (JY) et al., 2010; Luo et al., 2014; Shou et al., 2018; Zhao et al., 2015) and nutrient inputs from the groundwater discharge (Kim (JS) et al., 2010; Kim (G) et al., 2011). AN-D has increased in the CSK owing to industrial development in China during the last few decades, which has led to increased atmospheric N emission.

Data and Methods

Riverine N data

Hydrographic data from the MCH (Mechanisms Controlling Hypoxia – MCH Atlas) projects in the Gulf of Mexico were collected from the National Oceanographic Data Center (https://www.nodc.noaa.gov) covering the period from 2004 through 2007 (Table 1). We excluded cruises MCH M6 and M7 because the threat of hurricanes led to sampling different stations from the other cruises. The study sites and sampling areas are shown in Figure 1b. Quality control removed inconsistencies and anomalies in the data (e.g. removing outliers, missing data interpolation). Hydrographic data from the CSK (nutrients, salinity, oxygen) were collected during several cruises (Table 1 and Figure 1c and 1d), and the data were put through similar QA/QC routines.

Atmospheric Nitrogen Deposition (AN-D) data

Ocean Sci. Discuss., https://doi.org/10.5194/os-2019-46
Manuscript under review for journal Ocean Sci.
Discussion started: 20 May 2019

AN-D data from around the US are sparse (Table 2). Most US data have been collected along the east coast of the US and the only data in the GOM region were collected near Corpus Christi (~10 kg/ha/year; Wade and Sweet, 2008), Considerable AN-D could be expected, however, from the large number of petrochemical and fertilizer plants in southern TX, especially near Houston and along the Mississippi. While there are more data from the Yellow Sea (Kim (JY) et al., 2010; Luo et al., 2014; Shou et al., 2018; Zhao et al., 2015), they are still limited owing to the broad sampling coverage. While AN-D data in the Asian region were up to 140 kg/ha/year, data from the eastern side of the US were under 10 Kg/ha/year, even lower than in the GOM, suggesting there is currently not a large contribution from AN-D to total N loads to the North Atlantic Ocean. The approximate order of magnitude difference in AN-D concentrations between the GOM and the CSK is due to the continuing industrial development in East Asia and the resulting N emissions (Wang et al., 2016; Zhao et al., 2015).

Methodology: N-mass balance model

Our model consists of three sub-regions based on sampling locations during MCH cruises (Figure 3), each of which contains a series of one-quarter degree square boxes, as followed by Belabbassi (2006). The quarter degree boxes in this study were separated into an upper box and a lower box, based on pycnocline depth, as defined by a minimum change in oxygen concentration of 0.5 ml/L. We estimate potential production, which we count as an estimate of potential carbon flux (Figure 3a). Primary production (PP) above the pycnocline is expected to be higher than below it (Anderson 1969; Sigman and Hain, 2012), which means that the two layers have different biological processes. The difference in PP between upper and lower boxes also depends on the freshwater discharge rate, which determines nutrient input to the upper layer, seasonal variability,

Ocean Sci. Discuss., https://doi.org/10.5194/os-2019-46
Manuscript under review for journal Ocean Sci.
Discussion started: 20 May 2019

Ocean Science Discussions
Open Access

and transfer processes between the layers. While chlorophyll can be found below the pycnocline (DiMarco and Zimmerle, 2017), the fact that it is always associated with low oxygen concentrations suggests that it is not viable.

The N mass balance box model is modified from previous models to calculate the net removal of DIN inside each box, which represents potential primary production (PPP) (De Boer A.M. et al., 2010; Kim (G) et al., 2011) (Equation 1).

$$\boldsymbol{F^{DIN}_{Atmo}} + \left(\boldsymbol{C^{DIN}_{Box}} \times \boldsymbol{A_{Bott}} \times \boldsymbol{F_{River}}\right) + \boldsymbol{F^{DIN}_{Bott}} - \left(\boldsymbol{C^{DIN}_{EX}} \times \boldsymbol{V_S} \times \boldsymbol{\lambda_{Mix}}\right) = \boldsymbol{F^{DIN}_{Removal}} \quad \text{– Eq. 1}$$

where, $\boldsymbol{F^{DIN}_{Atmo}}$ is the flux from atmospheric nitrogen deposition, an input term. $\boldsymbol{C^{DIN}_{Box}}$ is the DIN concentration in each box, $\boldsymbol{A_{Bott}}$ is the bottom area of each quarter degree box, and $\boldsymbol{F_{River}}$ is river discharge rate. $\boldsymbol{F^{DIN}_{Bott}}$ is the benthic diffusion, another input term. The one quarter degree blue boxes located closest to the Mississippi and Atchafalaya river mouths were assumed to be the only ones affected by riverine input (Figure 3b). The output terms for water mixing are calculated from these factors; $\boldsymbol{C^{DIN}_{EX}}$ is the difference in DIN concentration between adjacent boxes, $\boldsymbol{V_S}$ is the water volume of each box, and $\boldsymbol{\lambda_{Mix}}$ is the mixing rate of each box. $\boldsymbol{F^{DIN}_{Removal}}$ is removal by biological production. The details of the model definitions are given below in Table 3 and shown in Figure 3. For instance, each arrow indicates input (blue) and output (red) terms (Figure 3). Input/output terms vary based on whether the boxes are above/below the pycnocline, while there are separate inputs from the Mississippi and Atchafalaya rivers.

The boxes above the pycnocline layer have two input terms; 1) Riverine N, which affects only a subset of boxes along the edge of each region, and 2) atmospheric nitrogen deposition (AN-D), which affects every box equally. The output terms are; 1) The exchange rate between each box (obtained by calculating different N concentrations between the east/west boxes and the on/offshore boxes), and 2) Removal by biological production, including sinking (assuming that any other removal factors are neglected). We tested the RC02 three zone hypothesis in the upper box layer, in which we can also examine the horizontal influence (horizontal extent) of the river plume based on production rates. In order to calculate the net removal of DIN in a box above the pycnocline layer, we used our N mass balance model in Equation 2.

$$F_{Atmo}^{DIN} + \left(C_{Box}^{DIN} \times A_{Bott} \times F_{River}\right) - \left(C_{EX}^{DIN} \times V_S \times \lambda_{Mix}\right) - F_{Sink}^{DIN} = F_{Removal}^{DIN} \quad \text{– Eq. 2}$$

However, below the pycnocline layer box, there are two input terms; 1) The benthic diffusion rate (defined here as diffusion from the groundwater and nutrient regeneration by bacteria in the sediment and bottom water; Nunnally et al., 2014), and 2) Vertical sinking from the box above the pycnocline layer, for which we used data from Qureshi (1995) while the output terms are; 1) the exchange rate between each box in the lower layer, and 2) upward transfer of dissolved material from the lower layer to the upper layer. Diffusion from groundwater can probably be ignored here as Rabalais et al. (2002) reported that the groundwater discharge is very low in coastal Louisiana, but is likely important elsewhere. Thus, in equation 3, the benthic diffusion rate is synthesized from existing literature results (Rowe et al., 2002; Nunnally et al., 2014), and multiplied by the area of each box and the decomposition rate. To calculate the net removal of DIN in boxes below the pycnocline layer, we used our N-mass balance model in Equation 3.

$$F_{Bott}^{DIN} + F_{Sink}^{DIN} - \left(C_{EX}^{DIN} \times V_S \times \lambda_{Mix}\right) = F_{Removal}^{DIN} \quad \text{– Eq. 3}$$

Ocean Sci. Discuss., https://doi.org/10.5194/os-2019-46
Manuscript under review for journal Ocean Sci.
Discussion started: 20 May 2019

Water transport in the region is generally from the east i.e., from near the Mississippi River in Sub-region A to the west, near the Atchafalaya River in Sub-region C during non-summer periods. During summer, the winds change direction from easterly to westerly, blocking the water flow to the west (Cho et al., 1998). We calculated advection from current meter data collected during the LATEX program (Nowlin et al., 1998a, b) from April 1992 to December 1994, from which we determined U (west to east flow) and V (south to north flow) components (cm s^{-1}). Figure 4 shows the mean values of coastal ocean current velocities. The annual range of the currents is 0 to 30 cm s^{-1} for the longshore component, with standard deviation of about 8 cm s^{-1}, and 0-7 cm s^{-1} for the cross-shelf component, with a similar standard deviation, but these current velocities are not constant and change depending on time and day. We used the mean value of the current velocity for the time of year during each cruise for calculating the advective flow factor in both alongshore and onshore/offshore directions.

To run the box model, we assumed four factors; 1) the study area is in a steady state condition, with equal input sources and outputs, 2) AN-D is evenly distributed across each area, 3) DIN is fully utilized by phytoplankton growth in the layer above the pycnocline, so we can neglect other removal factors, and 4) biomass, which is measured by chlorophyll data in this region, can be considered as equivalent to primary production (PP). We ignore denitrification below the pycnocline, which leads to a loss of nitrogen from the system, as large-scale anoxia is rare (Rabalais et al., 2007; Bianchi et al., 2010) and so our production numbers will likely be overestimated.

Because we assumed that this removed DIN is fully consumed by primary production, we can calculate potential carbon fluxes and oxygen consumption using the Redfield ratio (C: N: O: P = 106: 16: 138: 1). The PPP can be compared with ^{14}C measurement data (Lohrenz et al., 1998, 1999; Redalje et al., 1994; Quigg et al., 2011) and dissolved oxygen data from MCH mooring C at 29° N, 92° W (4/3/2005 ~ 7/10/2005) (Bianchi et al., 2010). Moreover, the PPP can be compared with estimated primary production (EPP) based on chlorophyll concentration data, assuming that we can make the conversion to carbon (e.g., using a chlorophyll to carbon ratio of 50: 1; Riemann et al., 1989).

Results

An N-mass balance model for the Texas-Louisiana Shelf

The existence of the three zones suggested by RC02 has been verified from winter data using nutrient/salinity relationships (Kim (JS) 2018). Figure 5 shows the contour graph based on the mean concentration of DIN at each station during the MCH M4 (March 2005) cruise. During summer, it is hard to use nutrient/salinity relationships directly because phytoplankton growth causes rapid nutrient consumption over the shelf, leading to low overall nutrient surface concentrations. We calculated the mean [DIN] in each box, and then used the relationship between DIN and salinity to define the edges of the three zones. Near the coast salinity was consistently low, with high turbidity from the river water discharge. This was labelled the brown (river) zone.

We used the N mass balance model to estimate PPP and carbon fluxes in the coastal GOM based on various N input sources. The PPP rates were highest near the river mouth and we set the boundaries of production for each zone based on our N mass balance model results and mean [DIN] data. We defined the PPP rate of the brown zone as being over 2 gC m^{-2} day^{-1} because of the high input of N from river, AN-D, and benthic diffusion and that in the blue zone as less than 0.1 gC m^{-2} day^{-1}. The PPP rate in the green zone is then between 0.1 and 2 gC m^{-2} day^{-1}.

Basically, these PPP ranges were set based on synthesized measured ranges of coastal GOM primary production, as defined for near, mid, and far fields of the coastal GOM (Dagg and Breed 2003; Lohrenz et al., 1999).

The edges of the three zones above and below the pycnocline layer, based on our N mass balance model results, are shown in Figures 6a and b. The boundaries above and below the pycnocline layer show different patterns for the edges of the zones. The brown zone was found above the pycnocline on all cruises close to the Mississippi River mouth because of the high nutrient concentrations, but only appeared off the Atchafalaya River in March 2005 (MCH M4). However, below the pycnocline it was found only in April 2004 (MCH M1) in sub-region A. This suggests that vertical transport across the pycnocline rapidly removes the high levels of suspended material that cause light limitation above the pycnocline. In the green zones, the nutrient source is mostly supported directly by the river, with minor additional sources of N from vertical sinking, AN-D, and benthic diffusion. We considered the vertical sinking flux based on sediment trap data from Qureshi (1995) below the pycnocline layer to estimate PPP. This varied between 0.1-1.0 $gN/m^2/d$ (Table 3). Typically, in the blue zone where biological production is low, vertical sinking followed by local decomposition is assumed to be the major factor to change the nutrient concentration in the lower layer. The blue zone is always more extensive below the pycnocline than above it, which suggests there is little or no production occurring except close to the coast and/or the river mouths, and agrees with the assumption that any chlorophyll below the pycnocline is inactive (Figure 6b). Thus, we can identify the horizontal influence of the river plume in the layer below the pycnocline and the variation in the boundaries of the three zones, based on the observed nutrient data from a bottom layer and our N mass balance model. The model suggests that regions of moderate potential productivity extend offshore at least as far as 28° 30’N in sub-

Ocean Sci. Discuss., https://doi.org/10.5194/os-2019-46
Manuscript under review for journal Ocean Sci.
Discussion started: 20 May 2019

region B, both above and below the pycnocline.

An N mass balance model calibration

The model calibration was done with historic literature data. Using observed chlorophyll data during the MCH cruises, we calculated the EPP using a carbon to chlorophyll ratio of 50: 1 (Riemann et al., 1989) to compare with results from previous researchers. Literature data suggest that PP rates in the green and brown zones of the coastal GOM vary between 0.4 gC m^{-2} day^{-1} (winter) and ~ 8 gC m^{-2} day^{-1} (summer) (Dagg et al., 2007; Lohrenz et al., 1998, 1999; Redalje et al., 1994). Quigg et al. (2011) found that the lowest integrated PP rates in 2004 (based on ^{14}C measurements) were on the outer part of the LATEX shelf (the blue zone) at 0.07 gC m^{-2} day^{-1} (in March), 0.04 ~ 0.15 gC m^{-2} day^{-1} (in May), and 0.33 ~ 0.91 gC m^{-2} day^{-1} (in July).

Table 4 compares our estimates of EPP and PPP using data from cruises MCH M1-M5 and M8. The difference between the EPP and PPP is that EPP was calculated from measured chlorophyll data, while PPP was calculated with our box model that assumes all nutrients were utilized by biological production. Note that in this study we assumed that all the chlorophyll concentration could be converted directly to production rates, which we considered as EPP. The EPP from cruises MCH M1 ~ M8 for samples from above the pycnocline calculated using our model is reasonable based on comparison with previous research PP values (Table 4). The highest EPP was found consistently in sub-region C, close to the Atchafalaya River input sources, while sub-region B showed the lowest EPP, apart from in May 2005. The EPP ranges were similar to previous ^{14}C measurement PP values of between 0.04 ~ 0.91 gC m^{-2} day^{-1}. Our calculated EPP were 0.28 ~ 0.48 gC m^{-2} day^{-1} in sub-region C, 0.11 ~ 0.25 gC m^{-2} day^{-1} in sub-region B, and 0.14 ~ 0.28 gC m^{-2} day^{-1} in sub-region A, respectively. Note that these ranges will

Ocean Sci. Discuss., https://doi.org/10.5194/os-2019-46
Manuscript under review for journal Ocean Sci.
Discussion started: 20 May 2019

Ocean Science Discussions
Open Access

vary depending on the carbon to chlorophyll ratio chosen. Based on our model calculation, which assumes all the nutrients are available for production, the PPP showed maxima at all times in sub-region A (near the Mississippi river) and minima in sub-region B (between the Mississippi and Atchafalaya River), except for MCH M2 in June 2004, when sub-region C had the lowest PPP (Table 4). The high values in sub-region A are due largely to underutilization of nutrients in regions of high turbidity. As the water flows west under the influence of the Coriolis effect, PPP is expected to decrease as a result of declining nutrient concentrations because of dilution and nutrient uptake during biological production while the water flows to sub-region B.

In sub-region C, MCH M4 (March 2005) had the highest PPP among the all MCH cruises. This probably depended on high nutrient concentrations being present during the winter period, when the region was affected by Atchafalaya River nutrient input.

Model scenarios in the Gulf of Mexico (GOM)

We tested the sensitivity of the model to changes in input/output parameters such as increasing AN-D and decreasing riverine N input. Assuming the model is robust, we investigated three model scenarios based on the nutrient distributions seen during the MCH1 cruise (note that using data from other cruises gives very similar results).. In the first scenario, we cut riverine N input 60% and increased the AN-D input by a factor of two based on increasing N emission predictions (Duce et al., 2008; He et al., 2010; Kanakidou et al., 2016; Kim (T) et al., 2011; Lawrence et al., 2000; Paerl et al., 2002). In the second scenario, we doubled the amount of AN-D as in scenario 1 and decreased riverine N input by 30% based on the hypoxia management plan goal (Gulf Hypoxia Action Plan Report, 2005, 2008; Rabalais et al. 2009). In the third scenario, we increased riverine N input by 20%, assuming the failure of the hypoxia management plan, while

Ocean Sci. Discuss., https://doi.org/10.5194/os-2019-46
Manuscript under review for journal Ocean Sci.
Discussion started: 20 May 2019

we set the AN-D amount equal with the first and second scenarios. Based on our N-mass balance model calculation and model scenarios, we can initially estimate carbon fluxes from our PPP rate, and, using the Redfield carbon to oxygen stoichiometry ratio (106:138), the overall oxygen balance within the coastal GOM (Table 5).

As can be seen in the scenario results for MCH M1 data (Table 5), the riverine N input source is still the major controlling factor in the coastal GOM region even when its contribution is greatly reduced and the AN-D source is doubled. For instance, if we fail to reduce riverine N input in future (scenario 3), the potential carbon fluxes will increase by 17% of current conditions results. In contrast, the AN-D input source only increased to a maximum of 5% of the total input term and this indicates that AN-D input is still a minor factor in the GOM. If the production is increased, overall oxygen demand will also be increased. The MCH M1 scenario result indicated that the overall oxygen demand would increase approximately 21% if we fail to reduce riverine N input, likely increasing considerably the area affected by hypoxia.

An N mass balance model in the Coastal Sea off Korea (CSK)

As we have done in the GOM, we used our N mass balance model to estimate the PPP in the MCK and define the three different zones (Figure 7). Similar to the GOM region, the PPP rates were highest near the river mouth, and we set the boundaries of each zone based on our N-mass balance model results. Based on nutrient data, as was done for the GOM, we defined the brown zone as having a PPP rate above 1.5 gC m^{-2} day^{-1} because of the high N sources from the river, AN-D, and benthic diffusion. We defined the green zone as having PPP rates between 0.3 to 1.5 gC m^{-2} day^{-1} and the blue zone as having rates of less than 0.3 gC m^{-2} day^{-1}.

The seasonal results shown in Figures 7a and b show that the boundaries of the three zones

Ocean Sci. Discuss., https://doi.org/10.5194/os-2019-46
Manuscript under review for journal Ocean Sci.
Discussion started: 20 May 2019

Ocean Science Discussions
Open Access

above and below the pycnocline layer were roughly consistent with the main change coming in summer (August), which is the wet season and sees the highest river discharge. The large size of the green zone in all seasons suggests that AN-D is consistently adding extra nitrogen to the surface ocean along with the riverine N input. This is supported by the fact that the PPP in the blue zone is an order of magnitude higher than for the GOM.

The AN-D input source comes mainly from the Chinese side of the East China Sea (ECS) and this affects the boundaries of the green and blue zones above the pycnocline as it is deposited uniformly across the region. There is also nutrient input from offshore, as the Yellow Sea Bottom Cold Water Mass can up-well during the mixing process and supply additional nutrients to the outer shelf (Lim et al., 2008).

Model scenarios in Mid-Western Coastal Sea off Korea (MCK)

AN-D is currently considerably more important (by approximately an order of magnitude) in the CSK than in the GOM), and it is anticipated that AN-D will likely be a major controlling factor here in the future (Duce et al., 2008; He et al., 2010; Kim (T) et al., 2011; Lawrence et al., 2000; Paerl et al., 2002).

Because of the lack of research on hypoxia scenario studies in Korea, we used the same three scenarios in the CSK as were used for the GOM. Similar to GOM results, riverine N input remains the major controlling factor, however, in this area, the AN-D source is more critical than in the GOM region (Table 6). The AN-D input source increased from 20% to 47% of the total input under scenario 1, while based on our scenario 3 results, increases in the AN-D input source and riverine N input together will affect biological production by increasing carbon fluxes up to 25% and oxygen demand up to 32% if we fail to reduce riverine N input in future (Table 6).

Ocean Sci. Discuss., https://doi.org/10.5194/os-2019-46
Manuscript under review for journal Ocean Sci.
Discussion started: 20 May 2019

Discussion

Most previous model studies were focused on predicting the hypoxia area in the GOM (Bierman et al., 1994; Fennel et al., 2011, 2013; Justic et al., 1996, 2002, 2003; Scavia et al., 2004). For example, Justic et al., (1996; 2003) used a two-layer model incorporating vertical oxygen data, from one station (LUMCON station C6; 28.867°N, 90.483°W), to predict the size of the hypoxia area. Similarly, Fennel et al. (2011; 2013) used her more complex simulation model, which included oxygen concentration as well as a plankton model from Fasham et al. (1990), to predict the size of the hypoxia region in the GOM. Our N mass balance model, in contrast, uses historical data from the LATEX shelf to estimate potential carbon fluxes in the GOM, and calculate the overall oxygen demand from those carbon fluxes. While this affects the total area subject to hypoxia it does not estimate the size of the hypoxic zone.

In contrast with our model, traditional predictive models have also ignored different nitrogen input sources such as AN-D and SGD. While this is probably reasonable on the Texas-Louisiana shelf, it may not apply in other coastal regions. As a result, model studies in this region have concluded that reducing riverine N input is the only solution to decrease the size of the hypoxia area in the GOM (Gulf Hypoxia Action Plan Report, 2005, 2008; Rabalais et al. 2009; Scavia et al., 2013). According to our model results, AN-D is still a minor controlling factor in the GOM, however, in the CSK, the AN-D contributed more to the total nitrogen budget and may be a major controlling factor in the future. This indicates that AN-D should be considered as another input term for nutrient managements, especially in Asia or in other regions where high concentrations are expected. Similarly, nitrogen input from either sediment diffusion or groundwater supply may also need to be considered.

Our zonal boundaries can be compared with the results of Lahiry (2007), who used

Ocean Sci. Discuss., https://doi.org/10.5194/os-2019-46
Manuscript under review for journal Ocean Sci.
Discussion started: 20 May 2019

salinity to define the edges of each zone for the three cruises MCH M1, M2, and M3 (Figure 8). Both sets of results showed good agreement near the Mississippi River regarding the boundaries of the brown and green zones, but less agreement near the Atchafalaya River region, our sub-region C. We believe that nutrient data are required to cover the complex biological processes that occur in the region, while the salinity relationship is more related to mixing between the fresh and offshore waters.

Both the GOM and CSK regions receive nitrogen inputs from AN-D, rivers, and benthic fluxes. These different nitrogen input sources control coastal productivity and this may reflect the different nitrogen cycling in the two regions. In the GOM, the riverine N input source consistently dominates coastal productivity and eutrophication, while, in the MCK, AN-D is also becoming a critical controlling factor. In the MCK, however, there is strong tidal mixing of freshwater from the Keum River and/or Gyunggi Bay with nearby coastal water, which results in a tidal front along the offshore region and off the Taean Peninsula during spring and summer. It is this physical mixing that mostly controls the spatial distribution patterns of nutrients and salinity here, particularly below the pycnocline (Lim et al., 2008). The brown zone in the upper layer in the MCK August 2008 cruise data changed to a green zone region below the pycnocline layer as a result of the strong coastal tidal mixing.

The results of our changing scenarios represent how the biological processes in these coastal regions are controlled by changes in individual sources of nutrients and show that in the near future both AN-D flux and riverine N flux need to be considered as regards nitrogen management of coastal waters. While our model cannot predict the area of the hypoxic zone, we can investigate the effects of potential flux changes of each factor, such as AN-D, riverine input, or benthic diffusion, and calculate the effects of changes in each on EPP (biomass) and on the

Ocean Sci. Discuss., https://doi.org/10.5194/os-2019-46
Manuscript under review for journal Ocean Sci.
Discussion started: 20 May 2019

overall oxygen balance for the region. We have only considered different input terms of our N mass balance model; output terms such as water mixing rates and the residence time for each box need more detailed study in future work to calculate more realistic production changes in each box.

Conclusion

We evaluated our model and tested its sensitivity based on three different scenarios. As a result, we believe that using our N mass balance model to separate different zones based on RC02 may be appropriate not only for large-scale regions like the GOM and MCK but also at small scales such as river or estuary systems. The model also estimates primary production and carbon flux based on inclusion of AN-D data that have not been considered previously (e.g. Bierman et al., 1994; Kim (T) et al., 2011). Our results agree well with previous ^{14}C measurements in the GOM (Quigg et al., 2011) and ocean color remote sensing in the MCK (Son et al., 2005).

Based on MCK cruise data results, we can initially determine where the three different zones are in the MCK. We identified the brown zone close to the Keum River mouth and the green and blue zones further away from the coast of Korea. Through our scenario results, we assume that the AN-D is a considerable factor in the MCK as well as the riverine N input from the Keum river.

These results show clearly that reducing nutrient inputs from the river is critical for the hypoxia management policy in the GOM (Gulf Hypoxia Action Plan Report, 2005, 2008; Rabalais et al. 2009). In addition, these model scenarios will be helpful in determining the direction of future coastal nutrient management or hypoxia management studies in the MCK, especially as AN-D sources become more important.

Ocean Sci. Discuss., https://doi.org/10.5194/os-2019-46
Manuscript under review for journal Ocean Sci.
Discussion started: 20 May 2019

Acknowledgements

The authors would like to thank to the captain and crew of the R/V Gyre along with the marine technicians and students who participated in the cruises. This project was funded by NOAA Center for Sponsored Coastal Ocean Research, Grant Numbers: NA03NOS4780039, NA06NOS4780198, and NA09NOS4780208.

References

Anderson, G. C.: Subsurface chlorophyll maximum in the northeast Pacific Ocean. Limnology and Oceanography., 14(3), 386-391, 1969.

Alexander, R. B., Smith, R. A., Schwartz, G. E., Preston, S. D., Brakebill, J. W., Srinivasan, R., and Pacheco, A. P.: Atmospheric nitrogen flux from the watersheds of major estuaries of the United States: An application of the SPARROW watershed model., 119-170, 2000.

Alexander, R. B., Smith, R. A., Schwarz, G. E., Boyer, E. W., Nolan, J. V., and Brakebill, J. W.: Differences in phosphorus and nitrogen delivery to the Gulf of Mexico from the Mississippi river basin. Environmental Science and Technology., 42, 822-830, 2008.

Belabbassi, L.: Examination of the relationship of river water to occurrences of bottom water with reduced oxygen concentrations in the northern Gulf of Mexico. Texas A & M University. Ph.D. Dissertation., 2006.

Bianchi, T. S., DiMarco, S. F., Cowan, Jr. JH., Hetland, R. D., Chapman, P., Day, J. W., and Allison, M. A.: The Science of hypoxia in the Northern Gulf of Mexico: A review. Science of the total Environment., 408(7), 1471-1484, 2010.

Bierman, V. J., Hinz, S. C., Wiseman, Jr. W. J., Rabalais, N. N., and Turner, R. E.: A Preliminary Mass Balance Model of Primary Productivity and Dissolved Oxygen in the Mississippi River Plume/Inner Gulf Shelf Region. Estuaries., 17(4), 886-899, 2004.

Bode, A., and Dortch, Q.: Uptake and regeneration of inorganic nitrogen in coastal waters influenced by the Mississippi River: spatial and seasonal variations. Journal of Plankton Resources., 18, 2251-2268, 1996.

Castro, M. S., Driscoll, C. T., Jordan, T. W., Reay, W. G., Boynton, W. R., Seitzinger, S. P., Styles, R. V., and Cable, J. E.: Contribution of atmospheric deposition to the total nitrogen loads to thirty-four estuaries on the Atlantic and Gulf coasts of the United States, 77–106, 2002.

Cho, K. R., Reid, O., and Nowlin, Jr W. D:. Objectively mapped stream function fields on the Texas-Louisana shelf based on 32 months of moored current meter data. Journal of Geophysics Research., 103(C5), 10377-10390, 1998.

Choi, H. Y., Lee, S. H., and Oh, I. S.: Quantitative Analysis of the Thermal Front in the Mid-Eastern Coastal Area of the Yellow Sea. Journal of the Korean Society of Oceanography [The Sea]., 3, 1-8, 1998.

Choi, H. Y., Lee, S. H., and Yoo, K. Y.: Salinity Distribution in the Mid-eastern Yellow Sea during the High Discharge from the Keum River Weir. Journal of the Korean Society of Oceanography [The Sea]., 4, 1-9, 1999.

Cornell, S., Rendell, A., and Jickells, T.: Atmospheric inputs of dissolved organic nitrogen to the oceans. Nature., 376, 243-246, 1995.

Dagg, M. J., and Breed, G. A.: Biological effects of Mississippi River nitrogen on the northern Gulf of Mexico-a review and synthesis. Journal of Marine Systems., 43, 133-152, 2003.

Dagg, M. J., Ammerman, J. W., AMON, R. M. W., Gardner, W. S., Green, R. E., Lohrenz, S. E.: A review of water column processes influencing hypoxia in the northern Gulf of Mexico. Estuaries Coasts., 30, 735-752, 2007.

De Boer, A. M., Watson, A. J., Edwards, N. R., and Oliver, K. I. C.: A multi-variable box model approach to the soft tissue carbon pump. Climate of the past., 6, 827-841, 2010.

Diaz, R. J., and Rosenberg, R.: Marine benthic hypoxia: A review of its ecological effects and the behavioural responses of benthic macrofauna. Oceanography Marine Biology. Ann. Rev., 33, 245-303, 1995.

Diaz, R. J., and Rosenberg, R.: Spreading dead zones and consequences for marine ecosystems. Science., 321(5891), 926-9, 2008.

DiMarco, S. F., and Zimmerle, H. M.: MCH Atlas: Oceanographic Observations of the Mechanisms Controlling Hypoxia Project. Texas A&M University, Texas Sea Grant, College Station, TX. Publication TAMU-SG- 17-601,350. ISBN 978-0-692-87961-0, 2017.

Dodds, W. K., and Smith, V. H.: Nitrogen, phosphorus, and eutrophication in streams. Inland Waters., 6, 155-164, 2016.

Doney, S. C., Mahowald, N., Lima, L., Feely, R. A., Mackenzie, F. T., Lamarque, J. F., and Rasch, P. J.: Impact of anthropogenic atmospheric nitrogen and sulfur deposition on ocean acidification and the inorganic carbon system. Proceedings of the National Academy of Science., 104, 14580-14585, 2007.

Dortch, Q., and Whitledge, T. E.: Does nitrogen or silicon limit phytoplankton in the Mississippi River plume and nearby regions? Continental Shelf Research., 12, 1293-1309, 1992.

Duce, R. A., LaRoche, J., Altierl, K., Arrigo, K. R., Baker, A. R., Capone, D. G., Cornell, S., Dentener, F., Galloway, J., Ganeshram, R. S., Geider, R. J., Jickells, T., Kuypers, M. M., Langlois, R., Liss, P. S., Liu, S. M., Middelburg, J. J., Moore, C. M., Nickovic, S., Oschlies, A., Pedersen, T., Prospero, J., Schlitzer, R., Seitzinger, S., Sorensen, L. L., Uematsu, M., Ulloa, O., Voss, M., Ward, B., and Zamora, L.: Impacts of Atmospheric Anthropogenic Nitrogen on the Open Ocean. Science., 320, 893-897, 2008.

Fasham, M. J. R., Ducklow, H. W., and Mckelvie, S. M.: A nitrogen-based model of plankton dynamics in the oceanic mixed layer. Journal of Marine research., 48 ,591-639, 1990.

Feng, Y., DiMarco, S. F., and Jackson, G. A.: Relative role of wind forcing and riverine nutrient input on the extent of hypoxia in the northern Gulf of Mexico. Geophysical Research Letters., 39, L09601, 2012.

Feng, Y., Fennel, K., Jackson, G. A., DiMarco, S. F., and Hetland, R. D.: A model study of the response of hypoxia to upwelling-favorable wind on the northern Gulf of Mexico shelf. Journal of Marine Systems., 131, 63-73, 2014.

Fennel, K., Wilkin, J., Levin, J., Moisan, J., O'Reilly, J., and Haidvogel, D.: Nitrogen cycling in the Middle Atlantic Bight: Results from a three-dimensional model and implications for the North Atlantic nitrogen budget. Global Biogeochemical cycles., 20, GB3007, doi:10.1029/2005G, 2006.

Fennel, K., Hetland, R. D., Feng, Y., and DiMarco, S. F.: A coupled physical-biological model of the Northern Gulf of Mexico shelf: model description, validation and analysis of phytoplankton variability. Biogeosciences., 8, 1881-1899, 2011.

Fennel, K., Hu, J., Laurent, A., Marta-Almeida, M., and Hetland, D. R.: Sensitivity of hypoxia predictions for the northern Gulf of Mexico to sediment oxygen consumption and model nesting. Journal of Geophysical Research: Oceans., 118, 990-1002, 2013.

Forrest, D. R., Hetlandl R. D., and DiMarco, S. F.: Multivariable statistical regression models of the areal extent of hypoxia over the Texas–Louisiana continental shelf. Environmental Research Letters., 6, 045002, 2011.

Goolsby, D. A. Mississippi basin nitrogen flux believed to cause Gulf hypoxia., EOS Transactions 2000:29–321, 2000.

Green, R. E., Gould, Jr. R. W., and Ko, D. S.: Statistical models for sediment/detritus and dissolved absorption coefficients in coastal waters of the northern Gulf of Mexico. Continental Shelf Research., 28(10), 1273-1285, 2008.

Gulf Hypoxia Action Plan Report. Mississippi River Gulf of Mexico Watershed Nutrient Task Force., 2005.

Gulf Hypoxia Action Plan Report. Mississippi River Gulf of Mexico Watershed Nutrient Task Force., 2008.

He, C. H., Wang, X., Liu, X., Fangmeler, A., Christie, P., and Zhang, F.: Nitrogen deposition and its contribution to nutrient inputs to intensively managed agricultural ecosystems. Ecological Application., 20(1), 80-90, 2010.

Hetland, R. D., and DiMarco, S. F.: How does the character of oxygen demand control the structure of hypoxia on the Texas-Louisiana continental shelf? Journal of Marine Systems., 70, 49-62, 2008.

Howarth, R. W., and Marino, R.: Nitrogen as the limiting nutrient for eutrophication in coastal marine ecosystems: Evolving views over three decades. Limnology and Oceanography., 51(1), 364-376, 2006.

Justic, D., Rabalais, N. N., and Turner, R. E.: Effects of climate change on hypoxia in coastal waters; A doubled CO2 scenario for the northern Gulf of Mexico. Limnology and Oceanography., 41(5), 992-1003, 1996.

Justic, D., Rabalais, N. N., and Turner, R. E.: Modeling the impacts of decadal changes in riverine nutrient fluxes on coastal eutrophication near the Mississippi River Delta. Ecological Modelling., 152, 33-46, 2002.

Justic, D., Rabalais, N. N., and Turner, R. E.: Simulated responses of the Gulf of Mexico hypoxia to variations in climate and anthropogenic nutrient loading. Journal of Marine Systems., 42, 115-126, 2003.

Kanakidou, M., Myriokefalitakis, S., Daskalakis, N., and Fanourgakis, G.: Past, Present, and Future Atmospheric Nitrogen Deposition. American Meteorological Society., 73(5), 2039-2047, 2016.

Kim, G., Kim, J. S., and Hwang, D. W.: Submarine groundwater discharge from oceanic islands standing in oligotrophic oceans: Implications for global production and organic carbon fluxes. Limnology and Oceanography., 56(2), 673-682, 2011.

Kim, J. S., Lee, M. J., Kim, J., and Kim, G.: Measurement of Temporal and Horizontal Variations in 222Rn Activity in Estuarine Waters for Tracing Groundwater Inputs. Ocean Science Journal., 45(4), 197-202, 2010.

Kim, J. S.: Implications of different nitrogen input sources for primary production and carbon flux estimates in coastal waters. Texas A&M University. Ph.D. Dissertation., 2018.

Kim, J. Y., Ghim, Y. S., Lee, S. B., Moon, K. C., Shim, S. G., Bae, G. N., and Yoon, S. C.: Atmospheric Deposition of Nitrogen and Sulfur in the Yellow Sea Region: Significance of Long-Range Transport in East Asia. Water, Air, and Soil Pollution., 205, 259-272, 2010.

Kim, T. W., Lee, K., Najjar, R. G., Jeong, H. D., and Jeong, H. J.: Increasing N abundance in the northwestern Pacific Ocean due to atmospheric nitrogen deposition. Science., 334, 505-509, 2011.

Lahiry, S.: Relationships between nutrients and dissolved oxygen concentrations on the Texas-Louisiana shelf during spring-summer of 2004. Texas A & M University. MS. Thesis., 2007.

Lawrence, G. B., Goolsby, D. A., Battaglin, W. A., and Stensland, G. J.: Atmospheric nitrogen in the Mississippi River Basin-emissions, deposition and transport. Science of The Total Environment., 248(2-3), 87-100, 2000.

Laurent, A., Fennel, K., Hu, J., and Hetland, R. D.: Simulating the effects of phosphorus limitation in the Mississippi and Atchafalaya River plumes. Biogeosciences., 9, 4797-4723, 2012.

Lim, D., Kang, M. R., Jang, P. G., Kim, S. Y., Jung, H. S., Kang, Y. S., and Kang, U. S.: Water Quality Characteristics Along Mid-Western Coastal Area of Korea. Ocean and Polar Research., 30(4), 379-399, 2008.

Liu, S. M., Zhang, J., Chen, S. Z., Chen, H. T., Hong, G. H., Wei, H., and Wu, Q. M.: Inventory of nutrient compounds in the Yellow Sea. Continental Shelf Research., 23, 1161-1174, 2003.

Lohrenz, S. E., Wiesenburg, D. A., Arnone, R. A., and Chen, X. G.: What controls primary production in the Gulf of Mexico? In: Sherman K, Kumpf H, Steidinger K (ed) The Gulf of Mexico Large Marine Ecosystem: Assessment, sustainability and management. Blackwell Science, Malden, MA., 151-170, 1998.

Lohrenz, S. E., Fahnenstiel, G. L., Redalje, D. G., Lang, G. A., Dagg, M. J., Whitledge, T. E., and Dortch, Q.: Nutrients, irradiance, and mixing as factors regulating primary production in coastal waters impacted by the Mississippi River plume. Continental Shelf Research., 19, 1113-1141, 1999.

Luo, X. S., Tang, A. H., Shi, K., Wu, L. H., Li, W. Q., Shi, W. Q., Shi, X. K., Erisman, J. W., Zhang, F. S., and Liu, X. J.: Chinese coastal seas are facing heavy atmospheric nitrogen deposition. Environmental Research Letters., 9, 1-10, 2014.

Milliman, J. D., and Meade, R. H.: World-wide delivery of river sediment to the oceans. The Journal of Geology., 91(1), 1-21, 1983.

Nipper, M., Sanchez Chavez, J. A., Tunnell, Jr. J. W.: “Marsh Island,” “Calcasieu Lake,” and “General Facts about the Gulf of Mexico.” GulfBase: Resource Database for Gulf of Mexico Research., 2004.

Nowlin, W. D. Jr., Jochens, A. E., Reid, R. O., and DiMarco, S. F.: Texas-Louisiana Shelf Circulation and Transport processes Study: Synthesis Report, Volume I: Technical Report. OCS Study MMS 98-0035. U.S. Dept. of the Interior, Minerals Mgmt Service, Gulf of Mexico OCS Region, New Orleans, LA., 502, 1998a.

Nowlin, W. D. Jr., Jochens, A. E., Reid, R. O., and DiMarco, S. F.: Texas-Louisiana Shelf Circulation and Transport processes Study: Synthesis Report, Volume II: Appendices. OCS Study MMS 98-0036. U.S. Dept. of the Interior, Minerals Mgmt Service, Gulf of Mexico OCS Region, New Orleans, LA., 288, 1998b.

Nunnally, C., Quigg, A., DiMarco, S. F., Chapman, P., and Rowe, G. T.: Benthic-Pelagic Coupling in the Gulf of Mexico Hypoxic Area: Sedimentary enhancement of hypoxic conditions and near bottom primary production. Continental Shelf Research., .85, 143-152, 2014.

Paerl, H. W., Dennis, R. L., and Whitall, D. R.: Atmospheric Deposition of Nitrogen: Implications for Nutrient Over-Enrichment of Coastal Waters. Estuaries., 25(4B), 677-693, 2002.

Paerl, H. W.: Controlling Eutrophication along the Freshwater-Marine Continuum: Dual Nutrient (N and P) Reductions are Essential. Estuaries and Coasts., 32, 593-601, 2009.

Park, M. J., Savenije, H. H. G., Cai, H., Jee, E. K., and Kim, N. H.: Progressive change of tidal wave characteristics from the eastern Yellow Sea to the Asan Bay, a strongly convergent bay in the west coast of Korea. Ocean Dynamics., 67, 1137-1150, 2017.

Park, Y. H.: Analysis of characteristics of Dynamic Tidal Power on the west coast of Korea. Renewable and Sustainable Energy Reviews., 68, 461-474, 2017.

Qureshi, N. A.: The role of fecal pellets in the flux of carbon to the sea floor on a river-influenced continental shelf subject to hypoxia. Louisiana State University. Ph.D. Dissertation., 1995.

Quigg, A., Sylvan, J., Gustafson, A., Fisher, T., Oliver, R., Tozzi, S., and Ammerman, J.: Going west: nutrient limitation of primary production in the northern Gulf of Mexico and the importance of the Atchafalaya River. Aquatic Geochemistry., 17, 519-544, 2011.

Rabalais, N. N , and Smith, L. E.: The effects of bottom water hypoxia on benthic communities of the southeastern Louisiana continental shelf. New Orleans, Louisiana, U.S. Minerals Management Service, Gulf of Mexico OCS Region.,105, 1995.

Rabalais, N. N., and Turner, R. E.: Hypoxia in the Northern Gulf of Mexico: Description, causes and change, pp. 1–36. In N. N. Rabalais and R. E. Turner (eds.), Coastal Hypoxia: Consequences for Living Resources and Ecosystems. Coastal and Estuarine Studies., 58, 2001.

Rabalais, N. N., Turner, R. E., and Scavia, D.: Beyond science into policy: Gulf of Mexico hypoxia and the Mississippi river. Bioscience. Vol.52(2). pp.129-142, 2002.

Rabalais, N. N., Turner, R. E., Sen Gupta, B. K., Boesch, D. F., Chapman, P., and Murrell, M. C.: Hypoxia in the northern Gulf of Mexico: Does the science support the plan to reduce, mitigate, and control hypoxia? Estuaries Coastal., 30, 753-772, 2007.

Rabalais, N. N., Turner, R. E., Justic, D., Diaz, R. J.: Global change and eutrophication of coastal waters. ICES. Journal of Marine Science., 66, 1528–1537, 2009.

Redalje, D. G., Lohrenz, S. E., and Fahnenstiel, G. L.: The relationship between primary production and the vertical export of particulate organic matter in a river impacted coastal ecosystem. Estuaries., 17, 829-838, 1994.

Riemann, B., Simonsen, P., and Stensgaard, L.: The carbon and chlorophyll content of phytoplankton from various nutrient regimes. Journal of Plankton Research., 11(5), 1037-1045, 1989.

Robertson, D. M., and Saad, D. A.: SPARROW Models Used to Understand Nutrient Sources in the Mississippi/Atchafalaya River Basin. Journal of Environmental Quality., 42, 1422-1440, 2014.

Rowe, G. T., and Chapman, P.: Hypoxia in the northern Gulf of Mexico: some nagging questions. Gulf Mexico Science., 20, 153-160, 2002.

Rowe, G. T., Kaegi, M. E. C., Morse, J. W., Boland, G. S., and Briones, E. G. E.: Sediment community metabolism associated with continental shelf hypoxia, northern Gulf of Mexico. Estuaries., 25(6), 1097–1106, 2002.

Scavia, D., Justic, D., and Bierman, V. J.: Reducing Hypoxia in the Gulf of Mexico: Advice from Three Models. Estuaries., 27(3), 419-425. 2004.

Scavia, D., Evans, M. A., and Obenour, D. R.: A scenario and forecast model for Gulf of Mexico hypoxic area and volume. Environmental Science and Technology., 47, 10423-10428, 2013.

Shou, W., Zong, H., Ding, P., and Hou, L.: A modelling approach to assess the effects of atmospheric nitrogen deposition on the marine ecosystem in the Bohai Sea, China. Esruarine, Coastal and Shelf Science., 208, 36-48, 2018.

Sigman, D. M., and Hain, M. P.: The Biological Productivity of the Ocean. Nature Education., 3, 1-16, 2012.

Son, S. H., Campbell, J. W., Dowell, M., Yoo, S. J., and Noh, J.: Primary production in the Yellow Sea determined by ocean color remote sensing. Marine Ecology Progress Series., 303, 91-103, 2005.

Sylvan, J. B., Dortch, Q., Nelson, D. M., Maier Brown, A. F., Morrison, W., Ammerman, J. W.: Phosphorus limits phytoplankton growth on the Louisiana shelf during the period of hypoxia formation. Environmental Science and Technology., 40(24), 7548– 7553, 2006.

Turner, R. E., and Rabalais, N. N.: Changes in the Mississippi River nutrient supply and offshore silicate-based phytoplankton community responses. In Dyer, K.R and R. J Orth(eds.). Changes in Fluxes in Estuaries: Implications from Science to management Proceedings of ECSA22/ERF Symposium. International Symposium Series. Olsen and Olsen. Gredensborg. Denmark.,147-150, 1994.

Turner, R. E., Rabalais, N. N., and Justic, D.: Predicting summer hypoxia in the northern Gulf of Mexico: riverine N, P and Si loading. Marine Pollution Bulletin., 51, 139-148, 2006.

Turner, R. E., Rabalais, N. N., and Justic, D.: Gulf of Mexico Hypoxia: Alternate States and a Legacy. Environmental Science and Technol., 42, 2323-2327, 2008.

Wade, T. L., and Sweet, S. T.: Final Report Coastal Bend Bays and Estuaries Program (CBBEP): Atmospheric Deposition Study., 48pp, 2008.

Wang, H., Dai, M., Liu, J., Kao, S. J., Zhang, C., Cai, W. J., Wang, G., Qian, W., Zhao, M., and Sun, Z.: Eutrophication-Driven Hypoxia in the East China Sea off the Changjiang Estuary. Environmental Science & Technology., 50, 2255-2263, 2016.

Yang, J. S., and Ahn, T. Y.: The analysis of the correlation between groundwater level and the moving average of precipitation in Kuem river watershed. The Journal of Engineering Geology., 18, 1-6, 2008.

Zhao, Y., Zhang, L., Pan, Y., Wang, Y., Paulot, F., and Henze, D. K.: Atmospheric nitrogen deposition to the northwestern Pacific: seasonal variation and source attribution. Atmos. Chem. Phys., 15, 10905-10924, 2015.

Ocean Sci. Discuss., https://doi.org/10.5194/os-2019-46
Manuscript under review for journal Ocean Sci.
Discussion started: 20 May 2019

Ocean Science Discussions
Open Access

List of Figures

Figure 1. Study sites and sampling areas in the GOM and Korea. Figure (a) shows the sampling area within the northern GOM, and (b) shows station positions from March 2005. Note that MCH project data are widely distributed across the region. Figure (c) shows the sampling area off the west coast of Korea and (d) shows all of the station positions.

Figure 2. The Rowe and Chapman three zone hypothesis, which described the physical and biochemical processes that initiate and sustain hypoxia on the Texas-Louisiana Shelf, [Rowe and Chapman, 2002]. Reprinted with permission of Gulf of Mexico Science

Figure 3. a. Input (blue) and output (red) sources for each 0.25° box (see text for details); b. Area of each sub-region (red) and boxes affected by direct riverine input (blue).

Figure 4. Mean ocean current velocities (a) and standard deviations (b) for biweekly periods from August 1993 through December 1994 based on data from LATEX project. Positive values of U show eastward flow; positive values of V show northward flow.

Figure 5. Extent of the three zones defined by RC02 based on the mean concentration of nutrient (DIN) at each station during the MCH M4 cruise in March 2005, showing their correspondence to the three sub-regions used in the box model. Red, brown and blue stations correspond to sub-regions A, B and C respectively.

Figure 6a. Areal distributions of the three zones using data from above the pycnocline, based on N mass balance model results. Colors and numbers represent boxes found in each of the three zones in terms of potential productivity (Unit: gC m^{-2} day^{-1}).

Figure 6b. As for 6a, using data from below the pycnocline.

Figure 7a. The distribution of the three zones off Mid-western Korea (MCK) above the pycnocline based on the RC02 hypothesis applied to the N mass balance model. Colors and numbers represent boxes found in each of the three zones in terms of potential productivity (Unit: gC m^{-2} day^{-1}).

Figure 7b. As for 7a, using data from below the pycnocline

Figure 8. Distribution of the three zones during cruises MCH M1-M3 based on salinity data (Lahiry, 2007). Areas shaded in three colors represent the brown, green and blue zones respectively.

Ocean Sci. Discuss., https://doi.org/10.5194/os-2019-46
Manuscript under review for journal Ocean Sci.
Discussion started: 20 May 2019

Ocean Science
Discussions

List of Tables

Table 1. Sampling dates for data from Gulf of Mexico projects and the coastal sea of Korea. Winter data are listed for the Gulf of Mexico cruises.

Table 2. Atmospheric Nitrogen Deposition (AN-D) in the USA and in the Yellow Sea.

Table 3. Definitions and values used in the N mass balance model to calculate DIN removal by biological production. (a) Each one quarter degree box; (b) Wade and Sweet 2008; (c) Qureshi 1995.

Table 4. Estimated primary production (EPP), which represent biomass and potential primary production (PPP) calculated from the upper layer box data. (Unit: gC m^{-2} day^{-1}).

Table 5. Simulation results for selected model scenarios based on MCH M1 (April 5-7, 2004), as described in the text. Biological production is calculated using our N-mass balance model, while oxygen demand is calculated by the Redfield stoichiometry ratio (C: O_2 = 106: 138). (Unit: gC m^{-2} day^{-1}).

Table 6. Simulation results for selected model scenarios based on CSK (February 2008) data, as described in the text. Biological production is calculated using our N-mass balance model, while oxygen demand is calculated by the Redfield stoichiometry ratio (C: O_2 = 106: 138). (Unit: gC m^{-2} day^{-1}).

Ocean Sci. Discuss., https://doi.org/10.5194/os-2019-46
Manuscript under review for journal Ocean Sci.
Discussion started: 20 May 2019

Ocean Science Discussions
Open Access
EGU

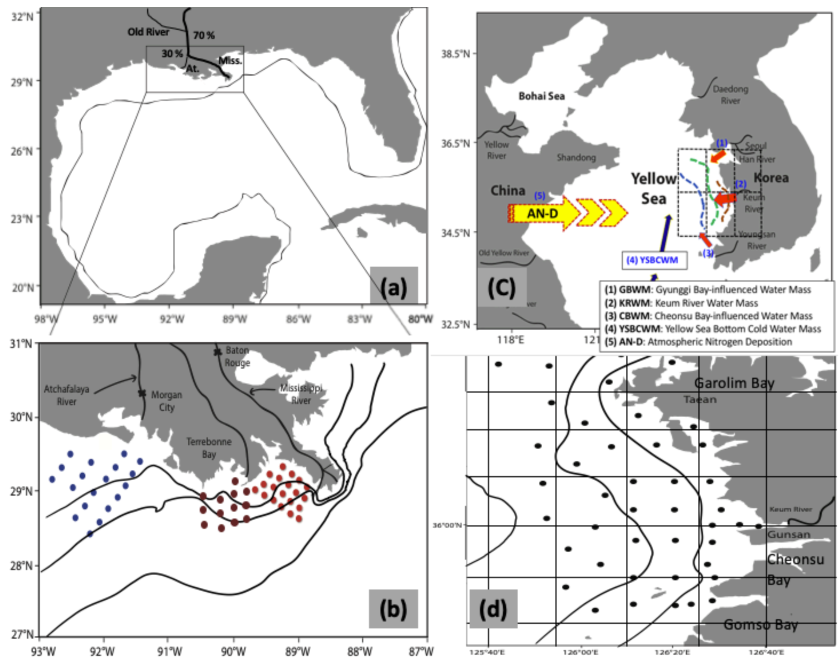

Figure 1. Study sites and sampling areas in the GOM and Korea. Figure (a) shows the sampling area within the northern GOM, and (b) shows station positions from March 2005. Note that MCH project data are widely distributed across the region. Figure (c) shows the sampling area off the west coast of Korea and (d) shows all of the station positions.

Ocean Sci. Discuss., https://doi.org/10.5194/os-2019-46
Manuscript under review for journal Ocean Sci.
Discussion started: 20 May 2019

Ocean Science
Discussions
Open Access

823 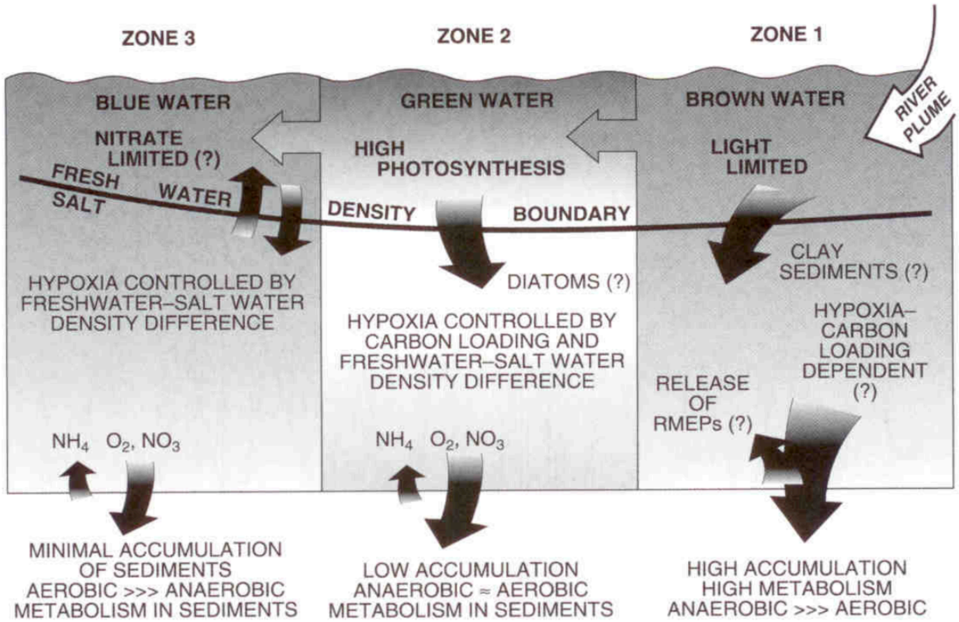

824 **Figure 2.** The Rowe and Chapman three zone hypothesis, which described the physical and
825 biochemical processes that initiate and sustain hypoxia on the Texas-Louisiana Shelf, [Rowe and
826 Chapman, 2002]. *Reprinted with permission of Gulf of Mexico Science.*

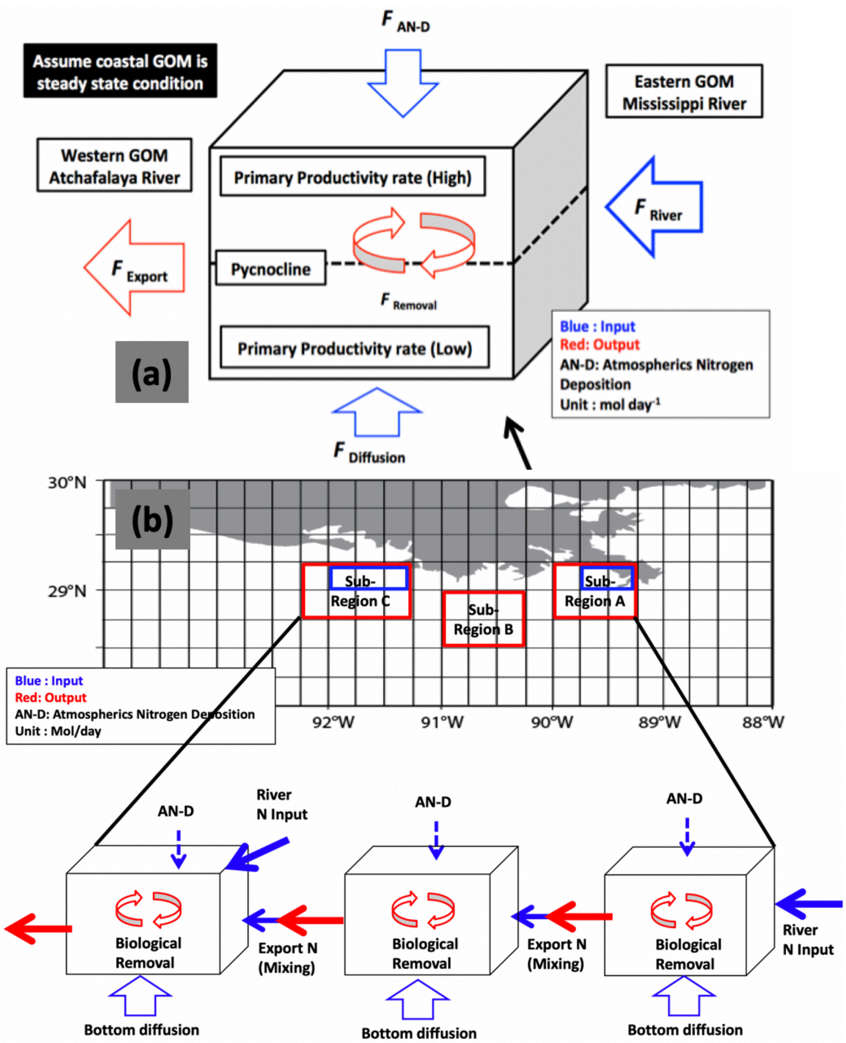

Figure 3. a. Input (blue) and output (red) sources for each 0.25° box (see text for details); b. Area of each sub-region (red) and boxes affected by direct riverine input (blue).

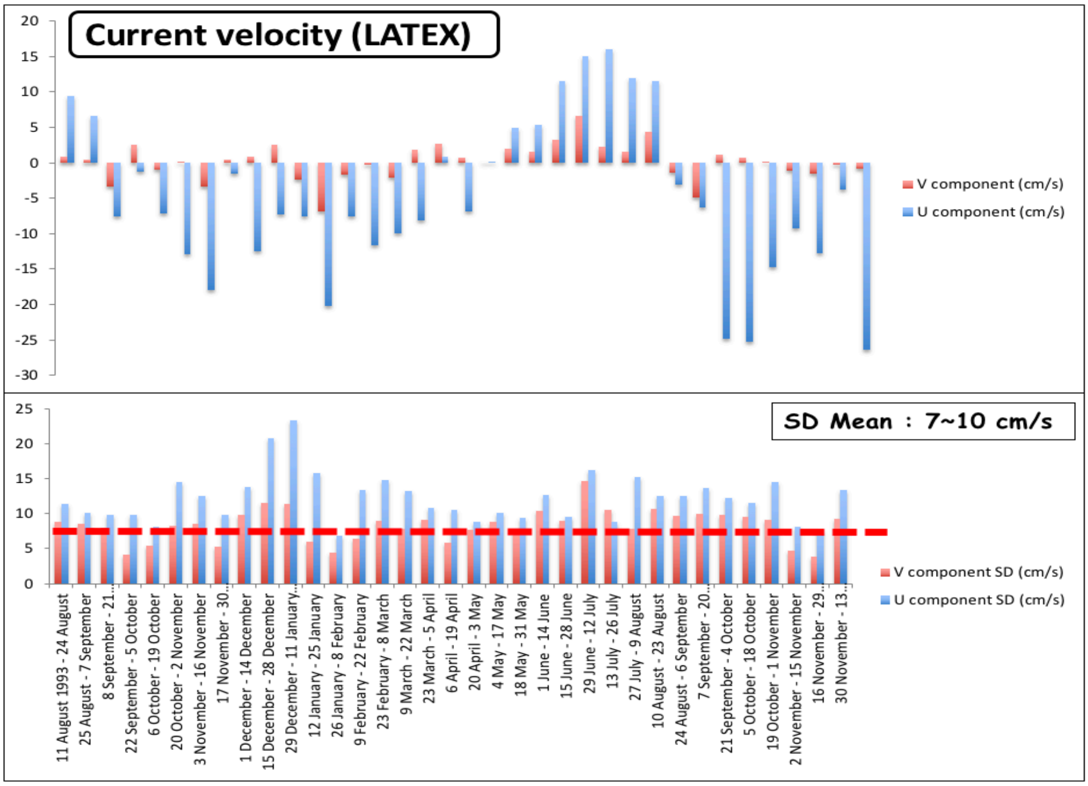

Figure 4. Mean ocean current velocities (a) and standard deviations (b) for biweekly periods from August 1993 through December 1994 based on data from LATEX project. Positive values of U show eastward flow; positive values of V show northward flow.

Ocean Sci. Discuss., https://doi.org/10.5194/os-2019-46
Manuscript under review for journal Ocean Sci.
Discussion started: 20 May 2019

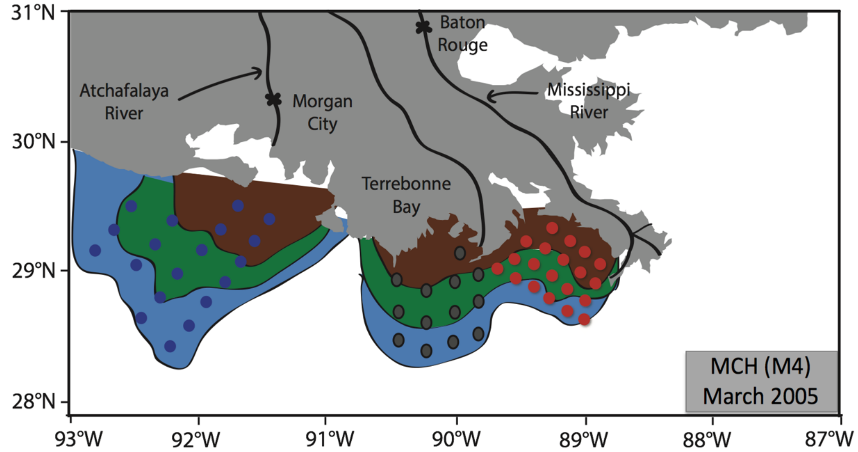

Figure 5. Extent of the three zones defined by RC02 based on the mean concentration of nutrient (DIN) at each station during the MCH M4 cruise in March 2005, showing their correspondence to the three sub-regions used in the box model. Red, brown and blue stations correspond to sub-regions A, B and C respectively.

Ocean Sci. Discuss., https://doi.org/10.5194/os-2019-46
Manuscript under review for journal Ocean Sci.
Discussion started: 20 May 2019

Ocean Science
Discussions
Open Access

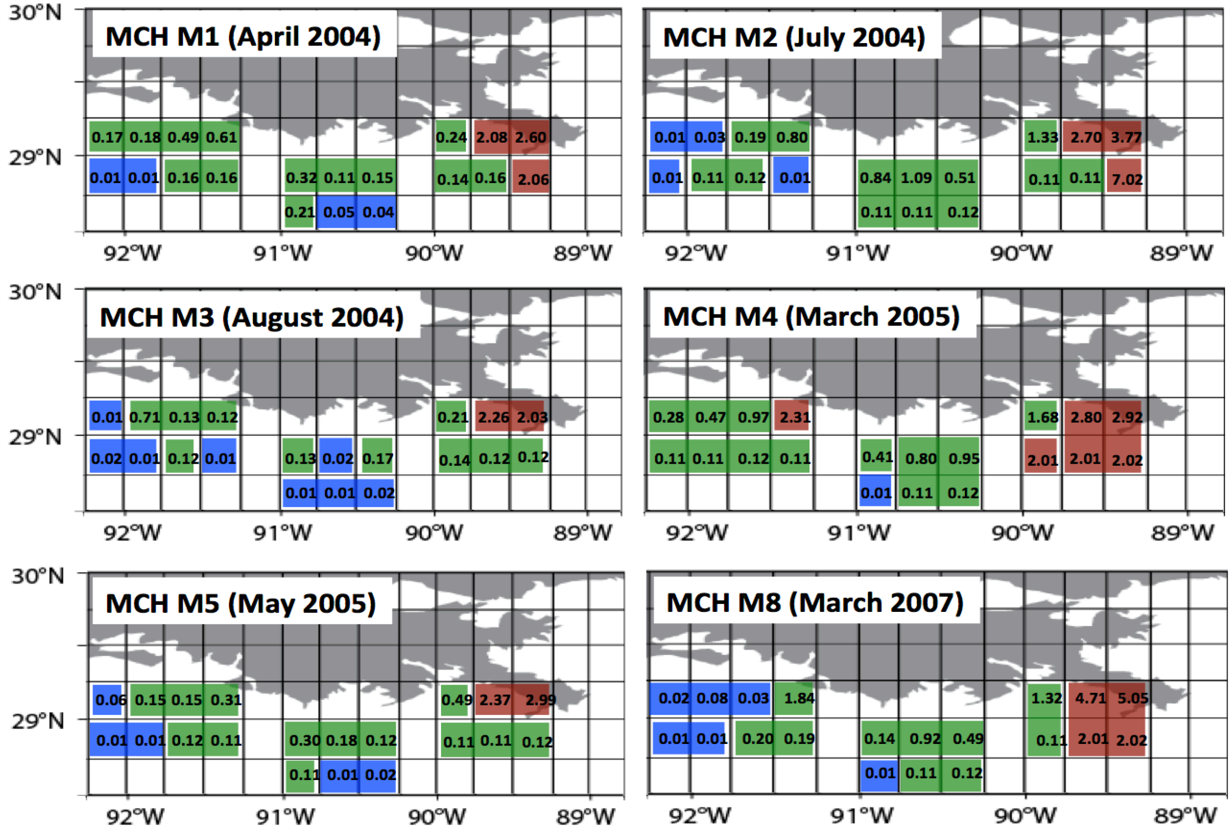

Figure 6a. Areal distributions of the three zones using data from above the pycnocline, based on N-mass balance model results. Colors and numbers represent boxes found in each of the three zones in terms of potential productivity (Unit: gC m^{-2} day^{-1}).

Ocean Sci. Discuss., https://doi.org/10.5194/os-2019-46
Manuscript under review for journal Ocean Sci.
Discussion started: 20 May 2019

Ocean Science
Discussions
Open Access

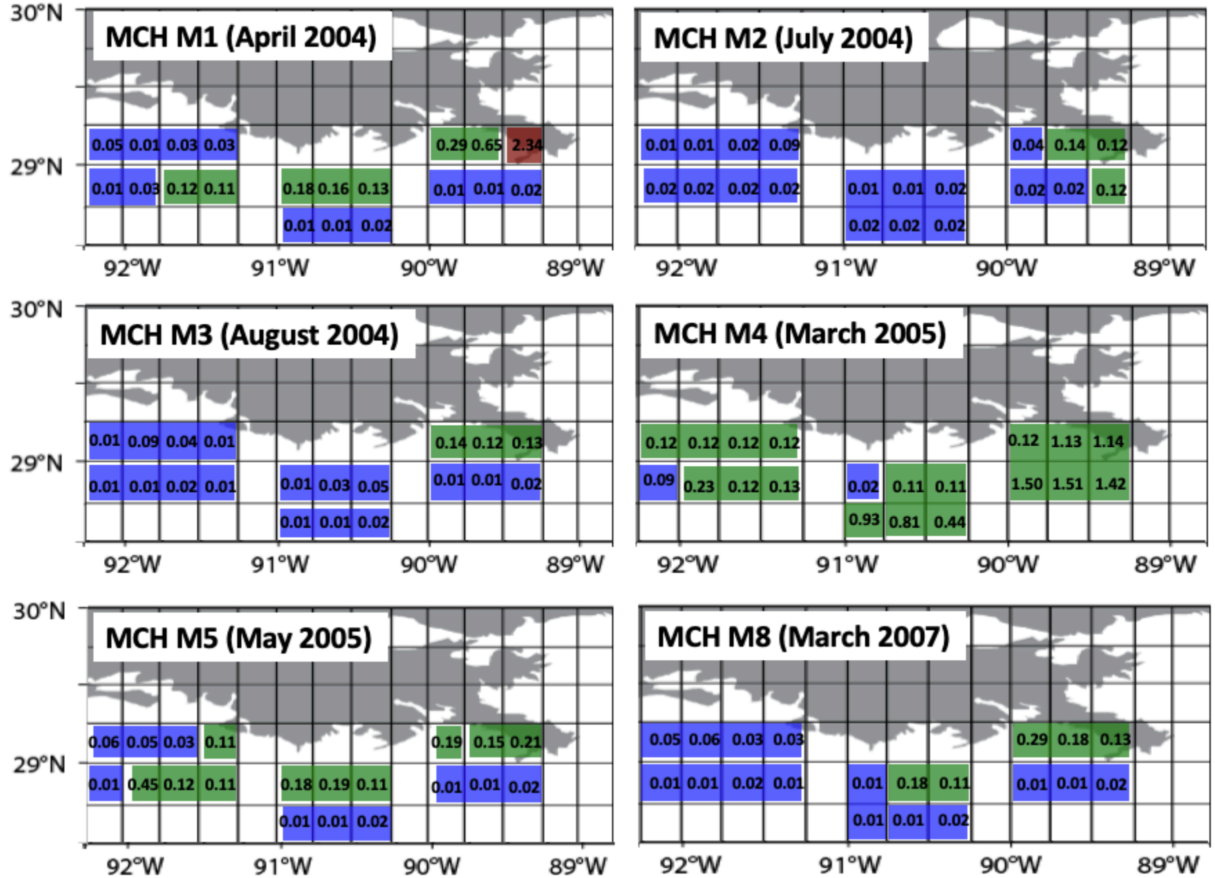

Figure 6b. As for 6a, using data from below the pycnocline.

Ocean Sci. Discuss., https://doi.org/10.5194/os-2019-46
Manuscript under review for journal Ocean Sci.
Discussion started: 20 May 2019

Ocean Science
Discussions
Open Access

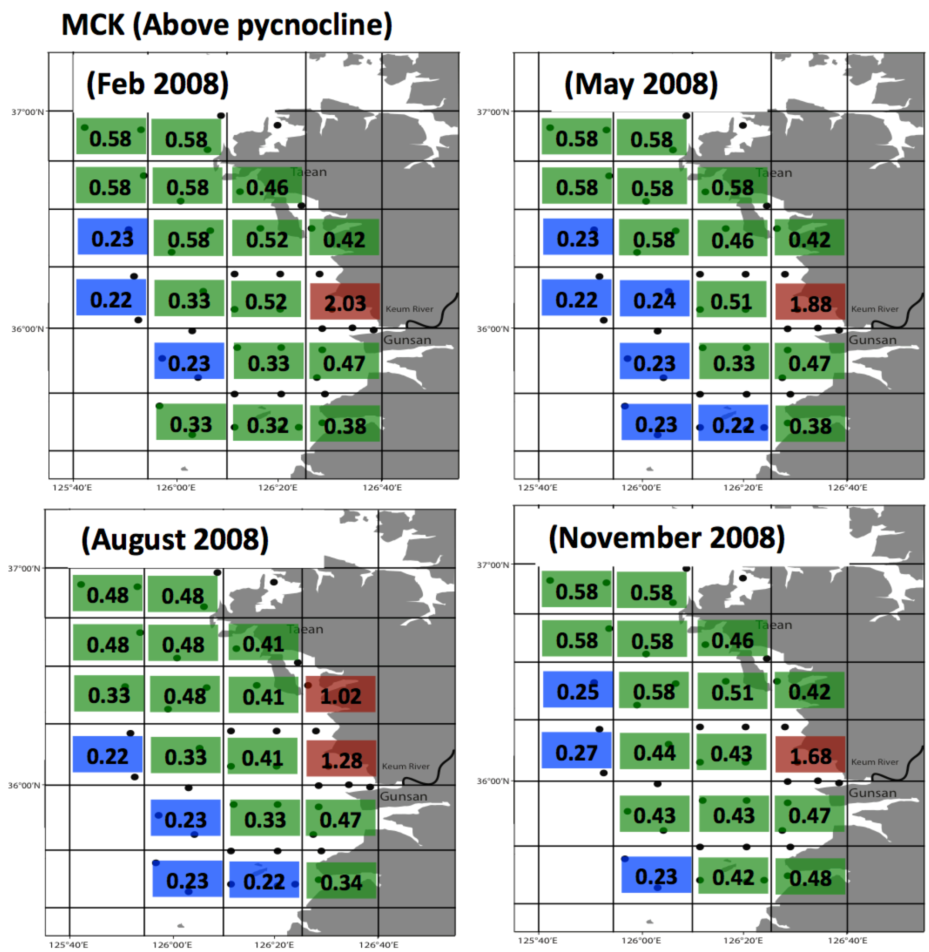

Figure 7a. The distribution of the three zones off Mid-western Korea (MCK) above the pycnocline based on the RC02 hypothesis applied to the N mass balance model. Colors and numbers represent boxes found in each of the three zones in terms of potential productivity (Unit: gC m^{-2} day^{-1}).

Ocean Sci. Discuss., https://doi.org/10.5194/os-2019-46
Manuscript under review for journal Ocean Sci.
Discussion started: 20 May 2019

Ocean Science
Discussions

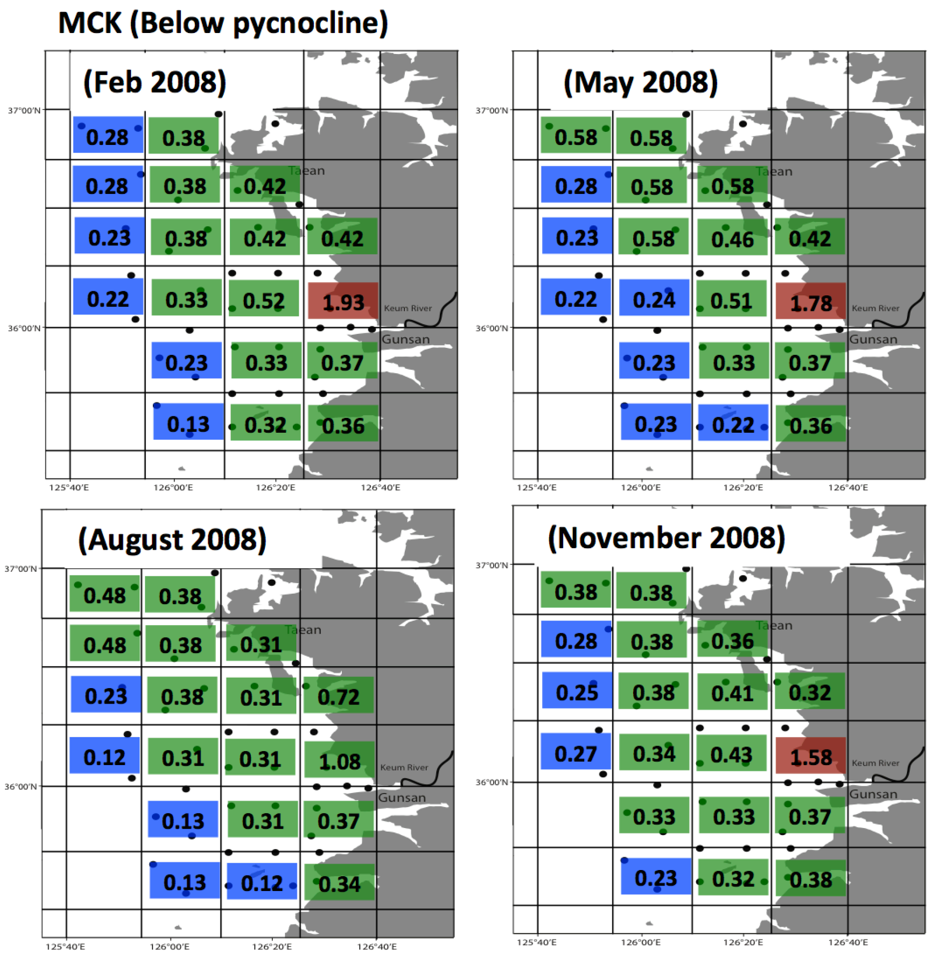

Figure 7b. As for 7a, using data from below the pycnocline.

Ocean Science
Discussions
Open Access

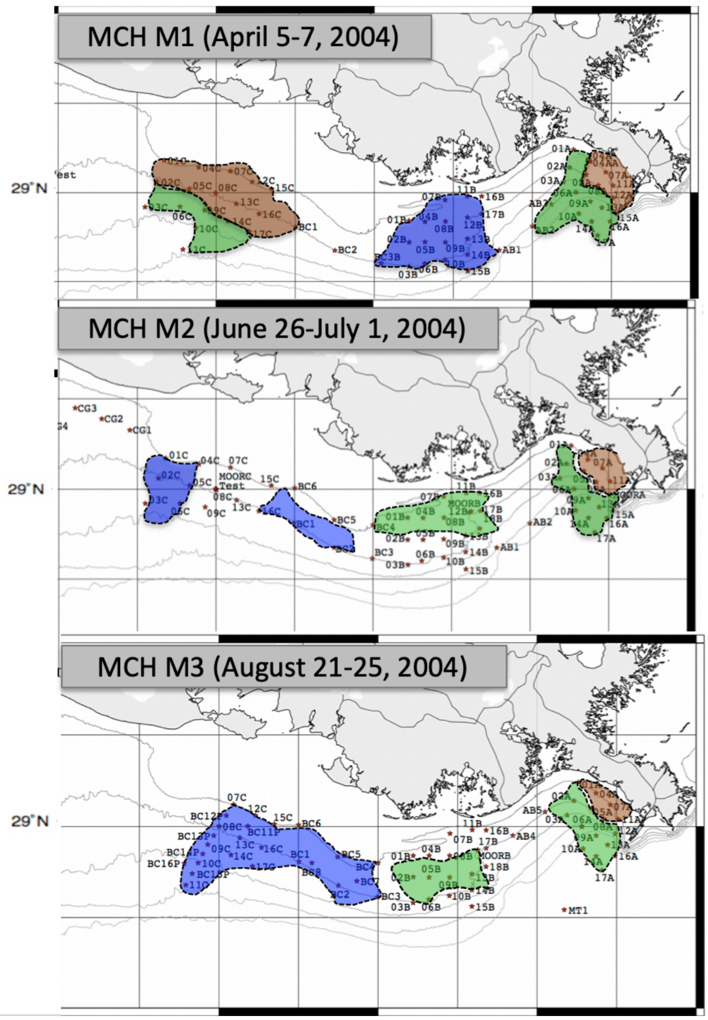

Figure 8. Distribution of the three zones during cruises MCH M1-M3 based on salinity data (Lahiry, 2007). Areas shaded in three colors represent the brown, green and blue zones respectively.

Ocean Sci. Discuss., https://doi.org/10.5194/os-2019-46
Manuscript under review for journal Ocean Sci.
Discussion started: 20 May 2019

Table 1. Sampling dates for data from Gulf of Mexico projects and the coastal sea of Korea. Winter data are listed for the Gulf of Mexico cruises.

Study area	Date	Cruise number
Gulf of Mexico MCH	April 5~7, 2004	MCH M1
	June 26~July 1, 2004	MCH M2
	August 21~25, 2004	MCH M3
	March 23~27, 2005	MCH M4
	May 20~26, 2005	MCH M5
	March 23~29, 2007	MCH M8
Korea MCK	Feb, May, Aug, Nov (2008)	

Ocean Sci. Discuss., https://doi.org/10.5194/os-2019-46
Manuscript under review for journal Ocean Sci.
Discussion started: 20 May 2019

Table 2. Atmospheric Nitrogen Deposition (AN-D) in the USA and in the Yellow Sea.

Watersheds	AN-D (Kg/ha/year)	References
Casco Bay, ME	1.5	Castro and Driscoll. 2002
Merrimack River, MA	1.2 ~ 4.0	Alexander et al. 2000
Long Island Sound, CT	1.8	Castro and Driscoll. 2002
Delaware Bay, DE	2.2 ~ 4.4	Castro and Driscoll. 2002 Goolsby. 2000
Chesapeake Bay	1.4 ~ 17.4	Alexander et al. 2000 Castro, M. S et al. 2000 Castro and Driscoll. 2002 Goolsby. 2000
Gulf of Mexico	10.0 ~ 11.5	Wade and Sweet. 2008
Bohai Sea	64.2 ~ 142.5	Shou et al. 2018
Yellow Sea (China on the west side)	16.1 ~ 18.4 29.9 ~ 32.8 38.1 ~ 92.4	Zhao et al. 2015 Luo et al. 2014 Shou et al. 2018
Yellow Sea (Korea on the east side)	15.0 ~ 58.2	Kim (JY) et al. 2010

Table 3. Definitions and values used in N-mass balance model to calculate DIN removal by biological production. (a) Each one quarter degree box; (b) Wade and Sweet 2008; (c) Qureshi 1995.

Unit	Definitions	Value
A_{Bott} (m^2)	Area of box	6.2 X 10^8 m^2 (a)
C_{Box}^{DIN} (μM)	DIN concentration in each area (box)	
V_S (m^3)	Water volume of box	A_{Bott} X Pycnocline depth
C_{EX}^{DIN} (mmol m^{-3})	Different concentration between each box **C_{EX}= (C_{On} - C_{Off}) or (C_{East} – C_{West}) for DIN**	
λ_{Mix} (day^{-1})	Mixing rate of each box to box (**A reciprocal of the water residence time**)	
F_{Atmo}^{DIN} (mol day^{-1})	Diffusive flux from Atmospheric deposition (Bulk N deposition rate x A_{Bott} ($A_{surface\ of\ ocean}$) for DIN	1.4 X 10^5 mol day^{-1} (b)
F_{Sink}^{DIN} (mol day^{-1})	Vertical sinking of DIN flux from sediment trap data	0.1 ~ 1 gN m^{-2} day^{-1} (c)
F_{River} (day^{-1})	River discharge	
F_{Bott}^{DIN} (mol day^{-1})	Benthic diffusion from the bottom sediments	
$F_{Removal}^{DIN}$ (day^{-1})	Removal by biological production (**Assuming that the other removal factors are negligible**)	

Ocean Sci. Discuss., https://doi.org/10.5194/os-2019-46
Manuscript under review for journal Ocean Sci.
Discussion started: 20 May 2019

Table 4. Estimated primary production (EPP), which represent biomass and potential primary production (PPP) calculated from the upper layer box data. (Unit: gC m^{-2} day^{-1}).

Cruise	**Sub-Region C**		**Sub-Region B**		**Sub-Region A**	
	EPP (Estimating Biomass)	**PPP**	**EPP** (Estimating Biomass)	**PPP**	**EPP** (Estimating Biomass)	**PPP**
MCH M1 (April 5-7, 2004)	0.28	0.22	0.23	0.15	0.23	1.21
MCH M2 (June 26-July 1, 2004)	0.48	0.19	0.11	0.46	0.14	2.50
MCH M3 (August 21-25, 2004)	0.33	0.17	0.15	0.06	0.16	0.81
MCH M4 (March 23-27, 2005)	0.33	0.71	0.15	0.40	0.28	2.24
MCH M5 (May 20-26, 2005)	0.30	0.12	0.25	0.12	0.18	1.03
MCH M8 (March 23-29, 2007)	0.36	0.33	0.17	0.30	0.18	2.54

Table 5. Simulation results for selected model scenarios based on MCH M1 (April 5-7, 2004). Biological production is calculated by our N-mass balance model. Oxygen demand is calculated by Redfield stoichiometry ratio (C: O_2 = 106: 138) (Unit: gC m^{-2} day^{-1}).

	F_{River}	$F_{AN\text{-}D}$	$F_{Bott/SGD}$	**Biological production**	**Oxygen demand**
Nominal Value	1.4×10^7 (~98 %)	1.4×10^5 (~1 %)	1.4×10^5 (~1 %)	Base line	
Scenario 1	5.6×10^6 (~93 %)	2.8×10^5 (~5%)	1.4×10^5 (~2%)	~45% decreased	~58% decreased
Scenario 2	9.8×10^6 (~96 %)	2.8×10^5 (~3%)	1.4×10^5 (~1%)	~22% decreased	~28% decreased
Scenario 3	1.7×10^7 (~97 %)	2.8×10^5 (~2%)	1.4×10^5 (~1%)	~17% increased	~21% increased

Ocean Sci. Discuss., https://doi.org/10.5194/os-2019-46
Manuscript under review for journal Ocean Sci.
Discussion started: 20 May 2019

Table 6. Simulation results for selected model scenarios based on CSK (February 2008) data. Biological production is calculated by our N-mass balance model. Oxygen demand is calculated by the Redfield stoichiometry ratio (C: O_2 = 106: 138) (Unit: gC m-2 day-1).

	F_{River}	$F_{AN\text{-}D}$	$F_{Bott/SGD}$	**Biological production**	**Oxygen demand**
Nominal Value	1.9×10^6 (~60%)	6.0×10^5 (~20%)	6.0×10^5 (~20%)	Base line	
Scenario 1	7.2×10^5 (~29%)	1.2×10^6 (~47%)	6.0×10^5 (~24%)	~13% decreased	~16% decreased
Scenario 2	1.3×10^6 (~41%)	1.2×10^6 (~39%)	6.0×10^5 (~20%)	~2% decreased	~2% decreased
Scenario 3	2.2×10^6 (~55%)	1.2×10^6 (~30%)	6.0×10^5 (~15%)	~25% increased	~32% increased